Electronic Supplementary Material (ESI) for Nanoscale.

Supporting Information

In situ total scattering experiments of nucleation and crystallisation of tantalum-based oxides: from highly dilute solutions via cluster formation to nanoparticles

Ezgi Onur Şahin,[a] Harun Tüysüz,[a] Candace K. Chan,[b,a] Gun-hee Moon,[a] Yitao Dai,[a] Wolfgang Schmidt,[a] Joohyun Lim,[c] Christina Scheu[c] and Claudia Weidenthaler *[a]

[a]Max-Planck-Institut für Kohlenforschung, Kaiser-Wilhelm-Platz 1, 45470 Mülheim an der Ruhr, Germany

[b]Materials Science and Engineering, School for Engineering of Matter, Transport and Energy (SEMTE), Arizona State University, Tempe, AZ 85287-8706, USA

[c]Max-Planck-Institut für Eisenforschung, Max-Planck-Straße 1, 40237 Düsseldorf, Germany

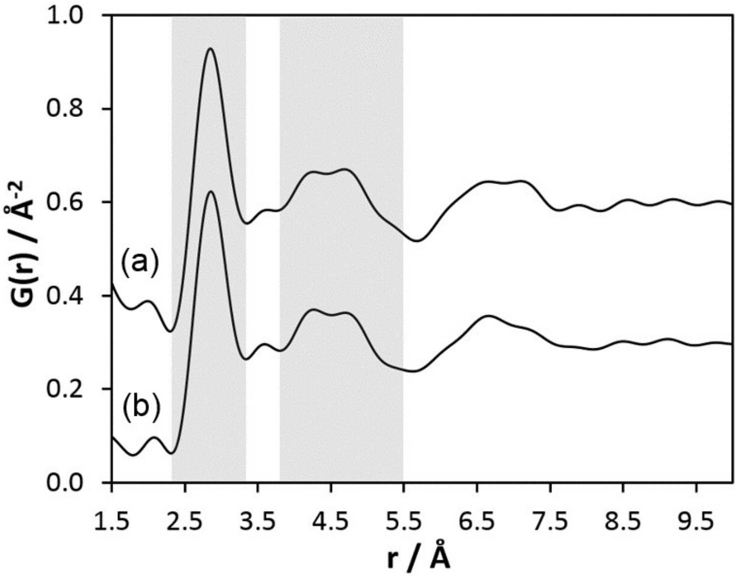

Fig. S1 Pair distribution functions (PDFs) of water-methanol mixture (a) flowing conditions and (b) static conditions. Data collected at the European Synchrotron Radiation Facility (ESRF), 90 keV (Q_{max}= 10 Å^{-1}).

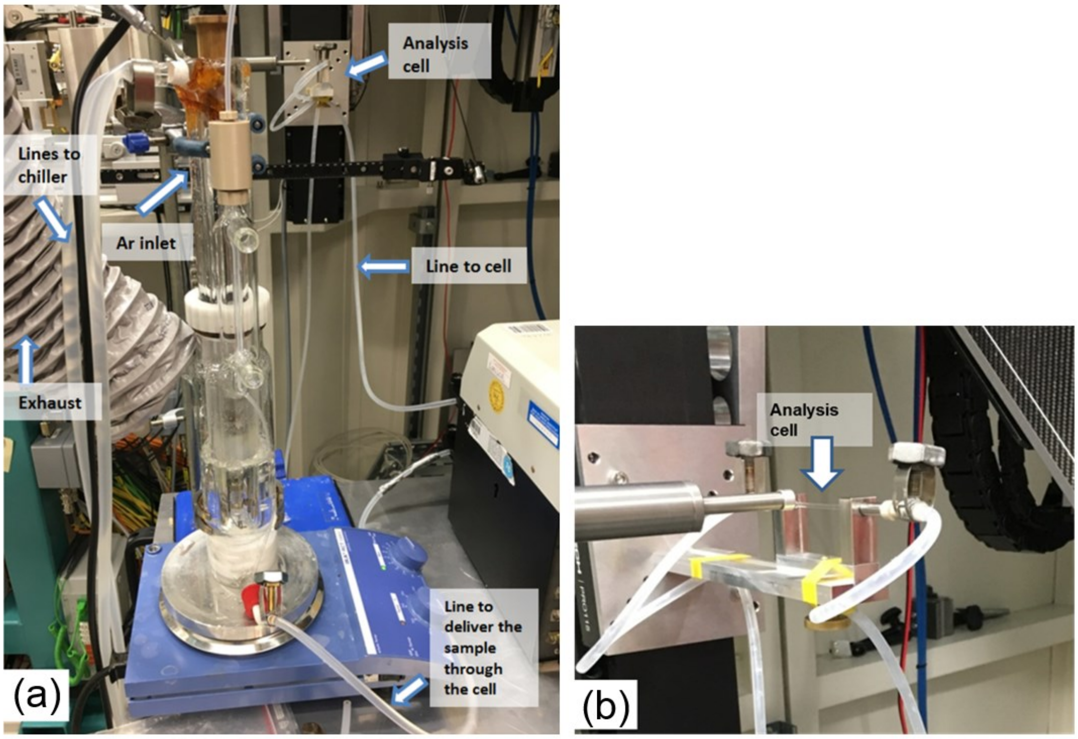

Fig. S2 Experimental setup used for synchrotron experiments. (a) The suspension in the glass reaction vessel is pumped through (b) the flow cell made of borosilicate glass in which the evolving particles are investigated with monochromatic X-rays for PDF analysis.

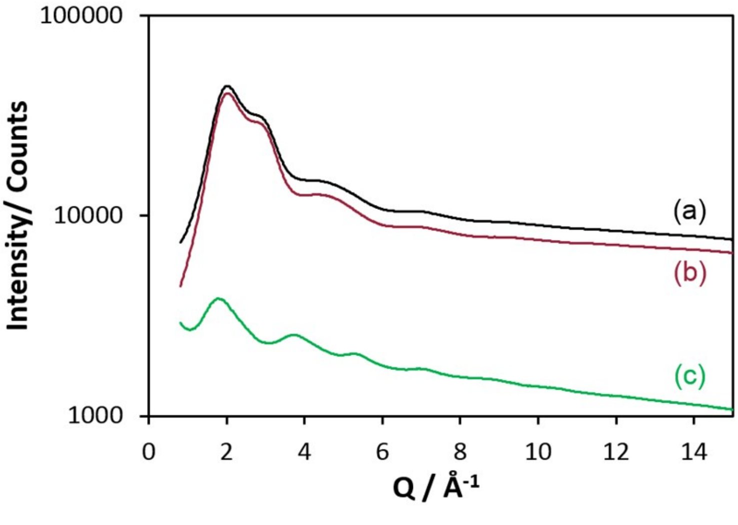

Fig. S3 Scattering data obtained at the ESRF, ID11 (a) after injection of $Ta_2(OEt)_{10}$ into water-methanol solution, (b) of water-methanol solution and (c) difference curve for which intensity is given on logarithmic scale. Dark current (electronic background noise) was subtracted from the data prior to subtraction of the scattering contribution of the water-methanol mixture from that of the $Ta(OEt)_5$ in water-methanol (resulting in the difference curve).

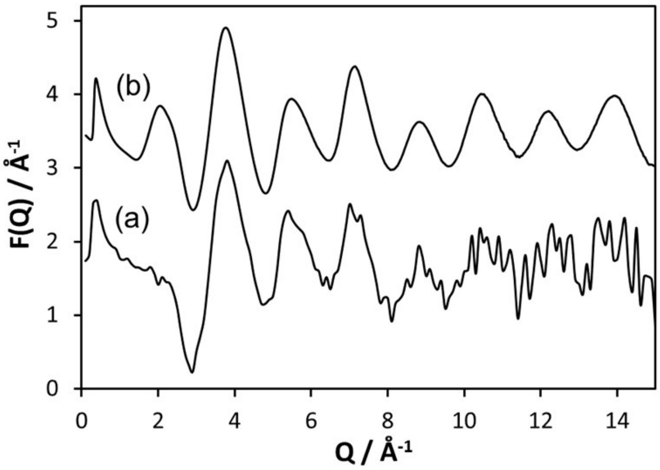

Fig. S4 F(Q) functions obtained from the scattering data collected for h-$Ta_xO_yH_z$ (a) in flow cell and (b) in capillary (static). Data collected at Diamond Light Source (Diamond), I15-1 (Q_{max}= 15 Å^{-1}).

As can be seen from Figure S4, the PDFs from the flow experiments are noisier than those from the static experiments. In the static case, the amorphous solid, which is usually evenly distributed within the complete volume of the liquid, tends to accumulate slightly more in the lower half of the capillary due to gravitation effects. In the static case, the X-ray beam was adjusted to pass through the accumulated precipitate. In that way, more solid was in the beam than in the flow case. The fact that sedimentation proceeds at all is due to the high specific density of the aggregated $Ta_xO_yH_z$ clusters containing tantalum with atomic number 73.

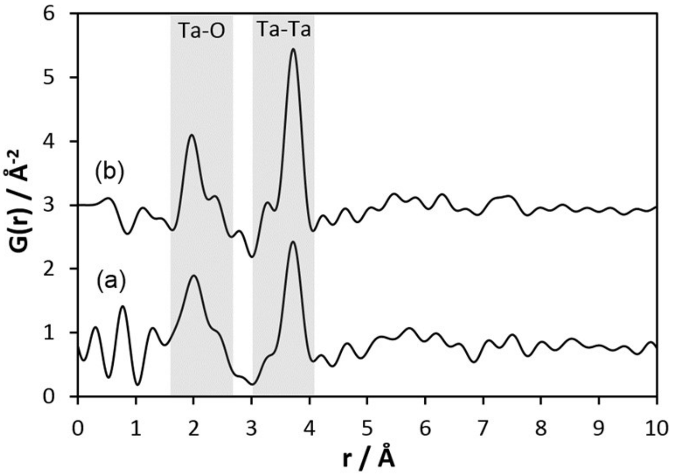

Fig. S5 PDFs obtained from the scattering data collected for h-$Ta_xO_yH_z$ (a) in flow cell and (b) in capillary (static). Data collected at Diamond, I15-1 (Q_{max}= 15 Å^{-1}).

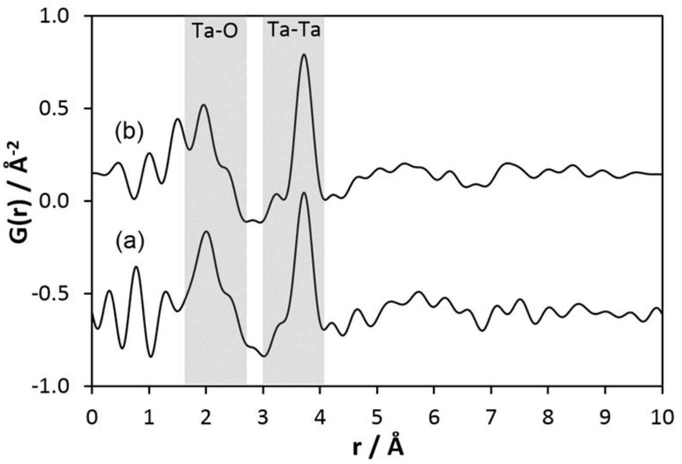

Fig. S6 PDFs obtained for h-$Ta_xO_yH_z$ from flow cell experiments performed at (a) Diamond, I15-1 and (b) at ESRF (Q_{max}= 15 $Å^{-1}$).

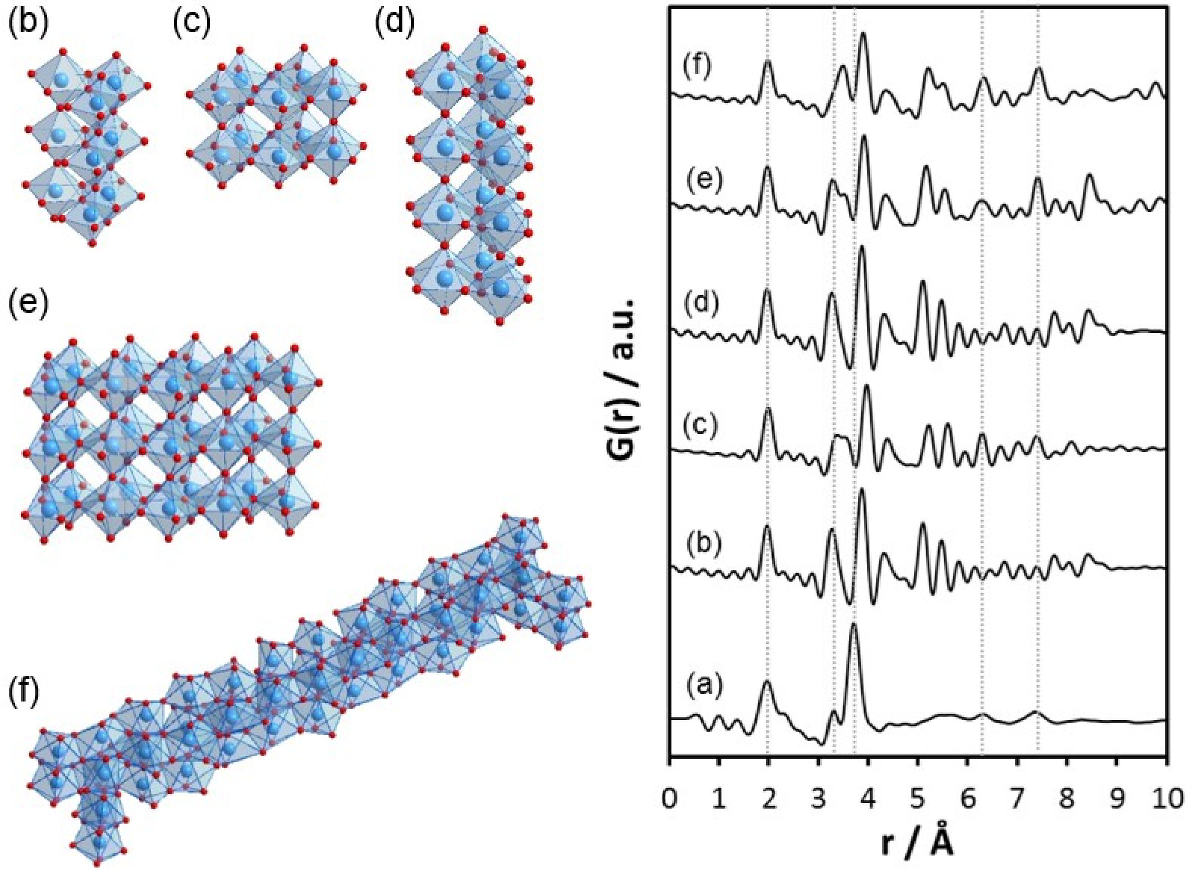

Fig. S7 Clusters cut out of the L-Ta_2O_5 structure[S1] (red and blue spheres represent O and Ta atoms respectively). (a) Experimental PDF obtained from h-$Ta_xO_yH_z$ is given in comparison to the PDFs calculated for (b) Ta_9O_{39}, (c) $Ta_{10}O_{43}$, (d) $Ta_{12}O_{51}$, (e) $Ta_{27}O_{108}$ and (f) $Ta_{50}O_{203}$ (Q_{max}= 20 $Å^{-1}$, delta2=1.0, sp-diameter=50 Å, Q_{damp}= 0.0258 $Å^{-1}$, Q_{broad}= 0.0118 $Å^{-1}$ using DebyePDFCalculator within Diffpy-CMI package[S2]).

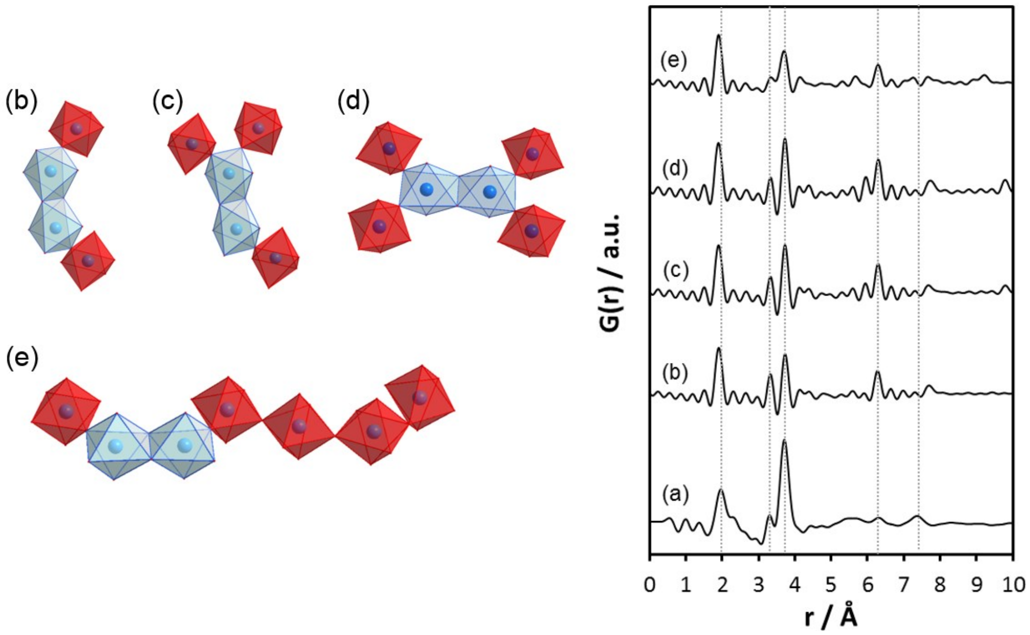

Fig. S8 Constructed chain-like clusters. (a) Experimental PDF obtained from h-$Ta_xO_yH_z$ is given in comparison to the PDFs calculated for the chain-like clusters (b) Ta_4O_{20}, (c) Ta_5O_{25}, (d) Ta_6O_{30} and (e) Ta_7O_{35} (Q_{max}= 20 $Å^{-1}$, delta2=1.0, sp-diameter=50 Å, Q_{damp}= 0.0258 $Å^{-1}$, Q_{broad}= 0.0118 $Å^{-1}$ using DebyePDFCalculator within Diffpy-CMI package[S2]).

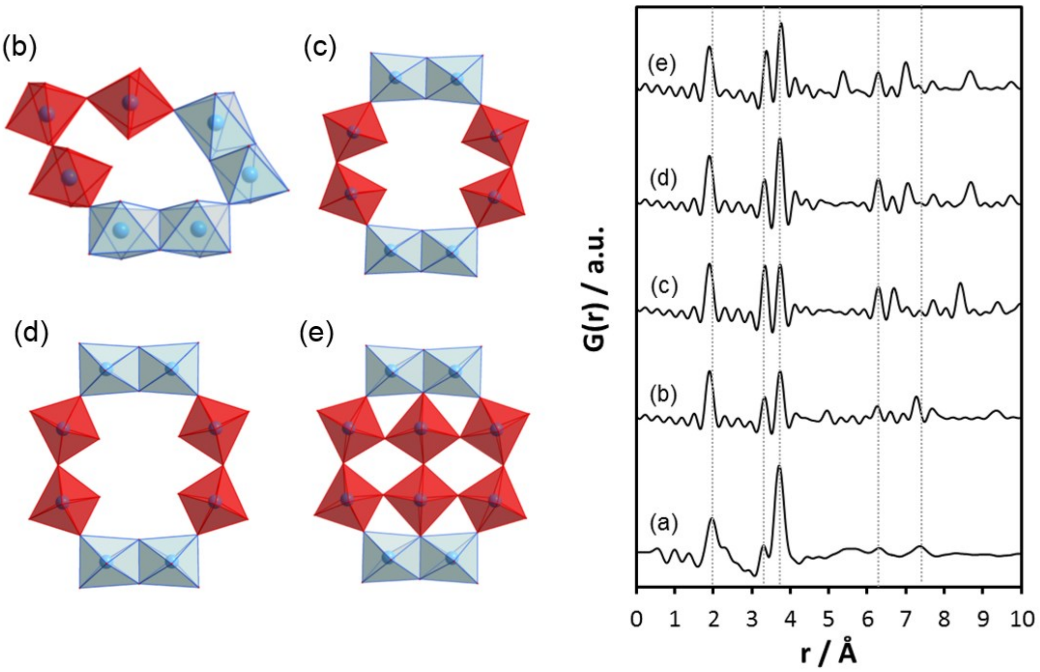

Fig. S9 Constructed ring-like clusters. (a) Experimental PDF obtained from h-$Ta_xO_yH_z$ is given in comparison to the PDFs calculated for the ring-like clusters (b) Ta_7O_{33}, (c) Ta_8O_{38}, (d) Ta_8O_{38} (slightly elongated along the major axis) and (e) $Ta_{10}O_{43}$ (Q_{max}= 20 $Å^{-1}$, delta2=1.0, sp-diameter=50 Å, Q_{damp}= 0.0258 $Å^{-1}$, Q_{broad}= 0.0118 $Å^{-1}$ using DebyePDFCalculator within Diffpy-CMI package[S2]).

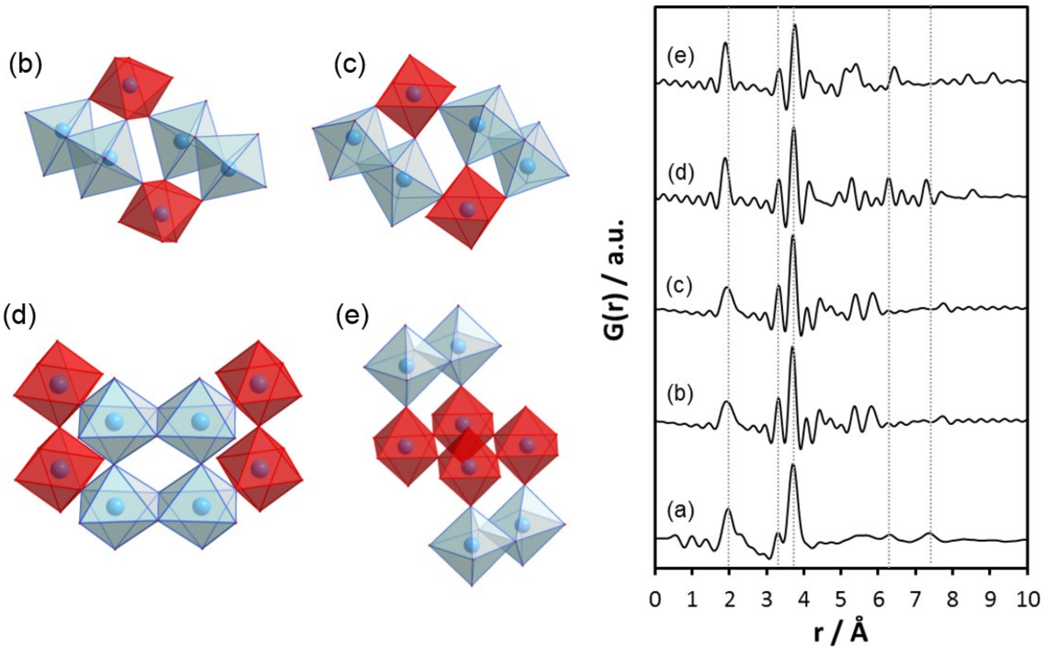

Fig. S10 Constructed clusters similarities with the model given by Abrahams.[S3] (a) Experimental PDF obtained from h-$Ta_xO_yH_z$ is given in comparison to the PDFs calculated for the clusters (b) Ta_6O_{26}, (c) Ta_6O_{26} (inner space widened), (d) Ta_8O_{36} and (e) Ta_8O_{36} (different arrangement) (Q_{max}= 20 Å^{-1}, delta2=1.0, sp-diameter=50 Å, Q_{damp}= 0.0258 Å^{-1}, Q_{broad}= 0.0118 Å^{-1} using DebyePDFCalculator within Diffpy-CMI package[S2]).

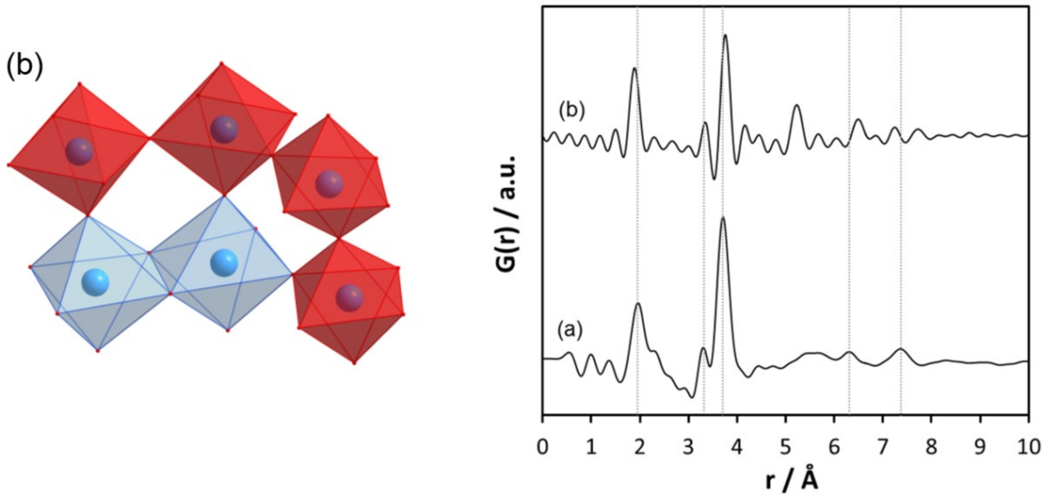

Fig. S11 Constructed model consisting of six octahedra two of which are edge-sharing. (a) Experimental PDF obtained from h-$Ta_xO_yH_z$ is given in comparison to (b) the PDF calculated for the cluster (Q_{max}= 20 Å^{-1}, delta2=1.0, sp-diameter=50 Å, Q_{damp}= 0.0258 Å^{-1}, Q_{broad}= 0.0118 Å^{-1} using DebyePDFCalculator within Diffpy-CMI package[S2]).

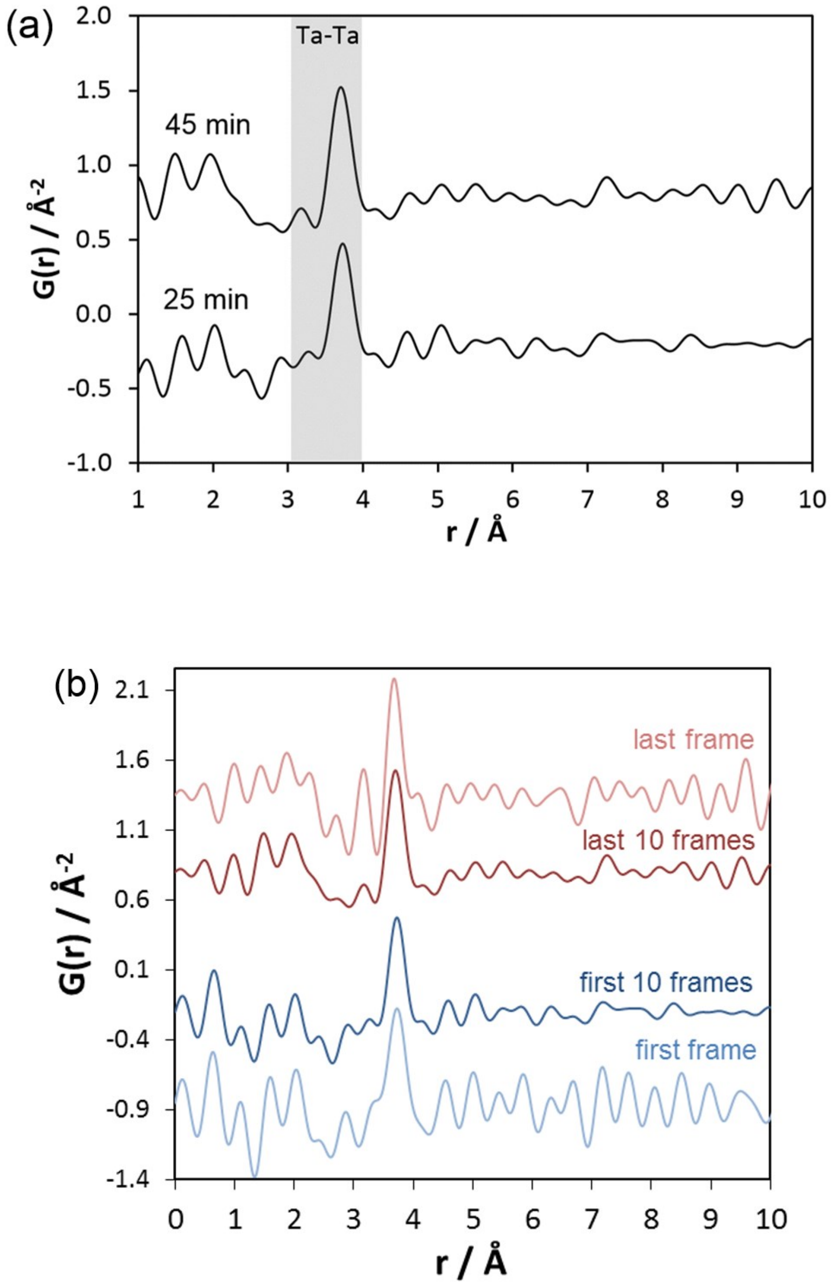

Fig. S12 *In situ* PDFs obtained from the scattering data collected for h-$Ta_xO_yH_z$ in the flow cell (a) by merging 10 collected data sets in I(Q) 25 min and 45 min after injection of the precursor. (b) PDFs obtained by merging first 10 and last 10 frames of the *in situ* experiment are compared to those generated from first and last single frames. Merging results in reduction of ripples in the PDFs. Data collection time per frame was 10 sec. Data collected at the ESRF, ID11 (Q_{max}= 15 Å^{-1}).

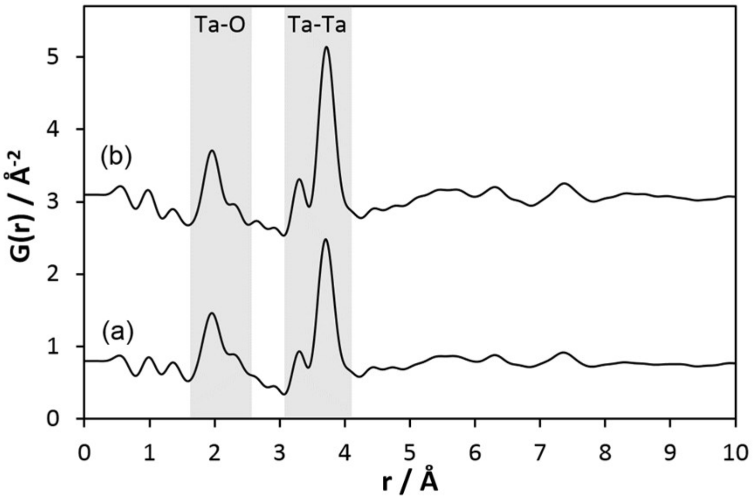

Fig. S13 PDFs obtained from the scattering data collected from (a) h-$Ta_xO_yH_z$ and (b) d-Ta_xO_y. Data collected at Diamond, I15-1 (Q_{max}: 20 Å^{-1}).

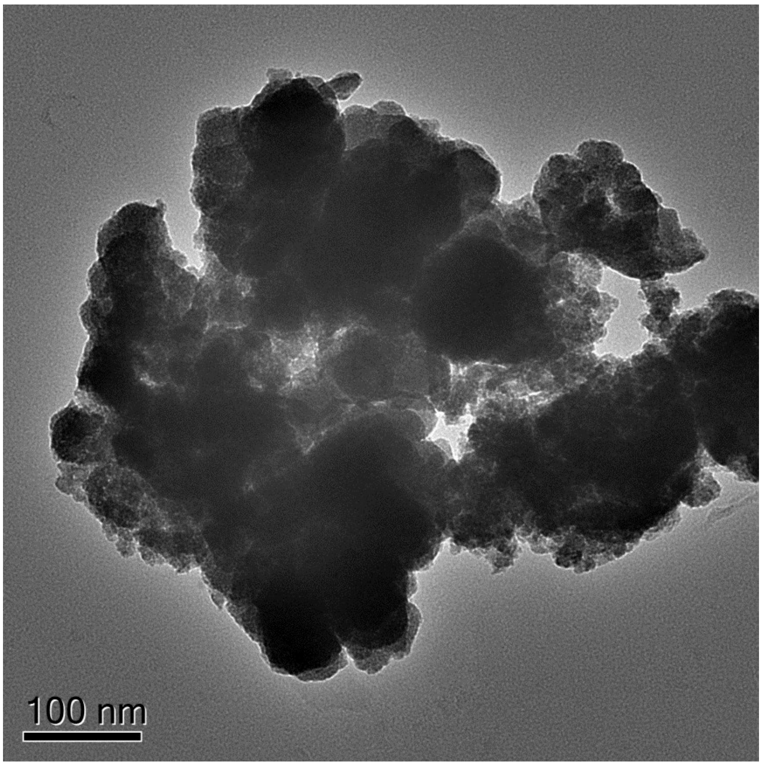

Fig. S14 Transmission electron microscopy image obtained from d-Ta_xO_y sample showing the aggregated morphology.

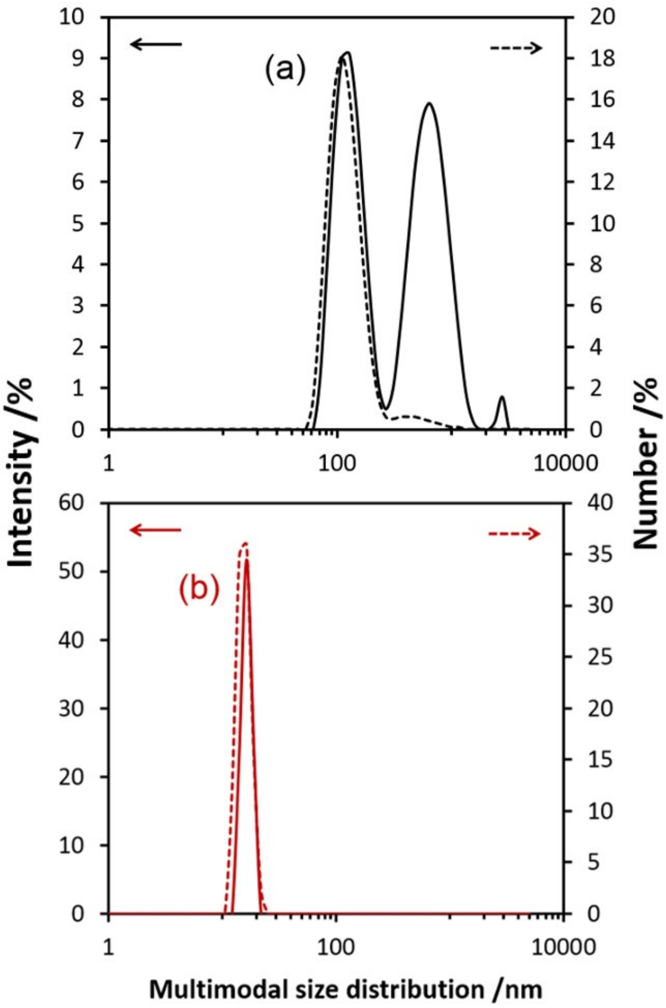

Fig. S15 Results of the dynamic light scattering obtained from h-$Ta_xO_yH_z$ (a) after centrifugation and ultrasonication and (b) after filtering. Solid lines show intensity percentage while dashed lines show number percentage of the particles. Note that the size values are plotted on logarithmic scale.

Complementary to structure analysis, thermogravimetry-differential scanning calorimetry (TG-DSC) experiments were used to identify crystallisation temperatures and functional groups in the amorphous d-Ta_xO_y. In TG-DSC experiments, d-Ta_xO_y was heated from room temperature to 950 °C under air flow applying different heating rates (to allow for determination of the activation energy for the crystallisation process). A first endothermic reaction between room temperature and 200 °C (Fig. S16a) was observed associated with a weight loss of about 10 %. Between 250 and 640 °C a broad signal belonging to an endothermic reaction was observed corresponding to a second weight loss. The first endothermic process is caused by the release of physisorbed water from the sample, while the second process corresponds to the release of water due to condensation of Ta-OH groups within the material. Crystallisation starts in the temperature range between 680 and 700 °C depending on the heating rate applied.

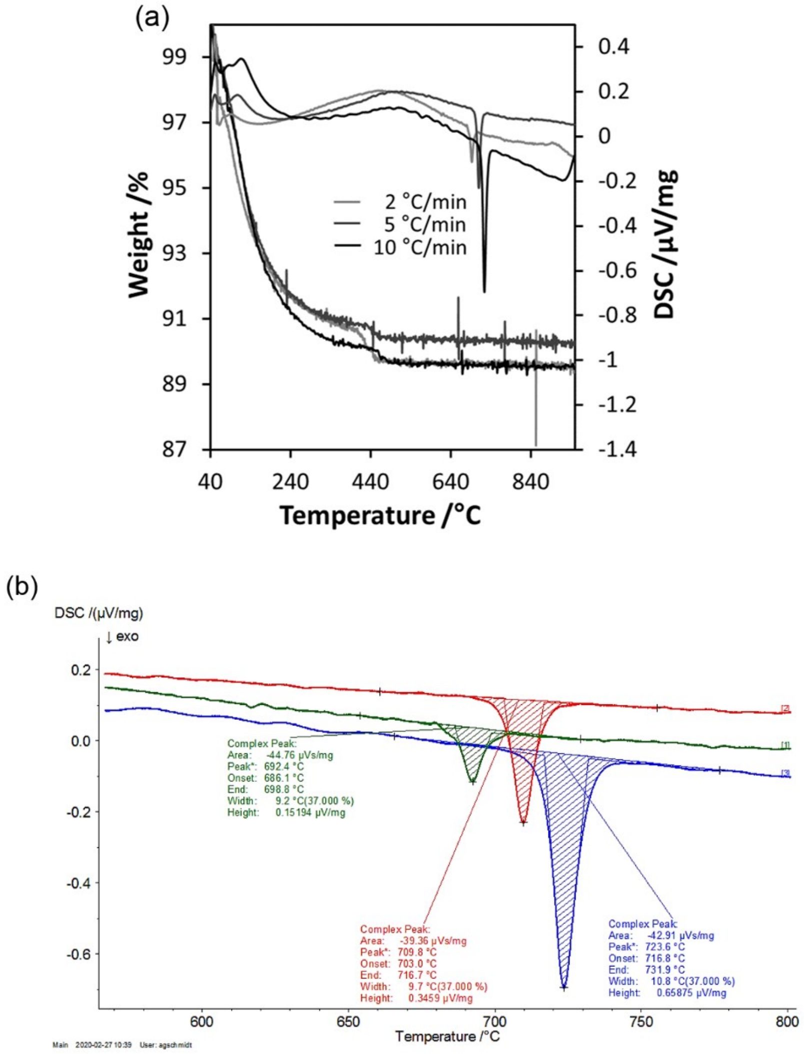

Fig. S16 (a) Differential scanning calorimetry (DSC) and thermogravimetric (TG) data obtained from d-Ta_xO_y sample and (b) features of the DSC peaks measured with heating rates 2 °C·min^{-1}(green), 5 °C·min^{-1}(red) and 10 °C·min^{-1}(blue) in air.

From the maxima of the DSC signals measured at different heating rates (Fig. S16b), the activation energy for the crystallisation process can be determined from a Kissinger plot.[S4] H. Kissinger developed a method allowing determination of the activation energy (E_a) for first order reactions from DTA or DSC data measured with a set of different heating rates (ϕ). Kissinger based his method on an equation reported by Murray and White[S5], i.e.:

$$Ae^{-\frac{E_a}{RT_m}} = \frac{E_a}{RT^2{}_m}\frac{dT}{dt}$$

where T_m is the peak maximum of the maximum (or minimum) value of a DTA or DSC peak caused by the respective reaction, dT/dt = ϕ the heating rate, R the gas constant, and A the frequency factor (probability that a molecule having the energy *E* will participate the reaction).

From that formula it can be seen that:

$$ln\frac{\phi}{RT^2{}_m} = -\frac{E_a}{R}\frac{1}{T_m} + ln\left(\frac{A}{E_a}\right)$$

Thus, plotting $\ln(\phi/T_m^2)$ versus $1/T_m$ will yield $-E_a/R$ as the slope of the curve. Multiplying the slope with R then will give the activation energy E_a.

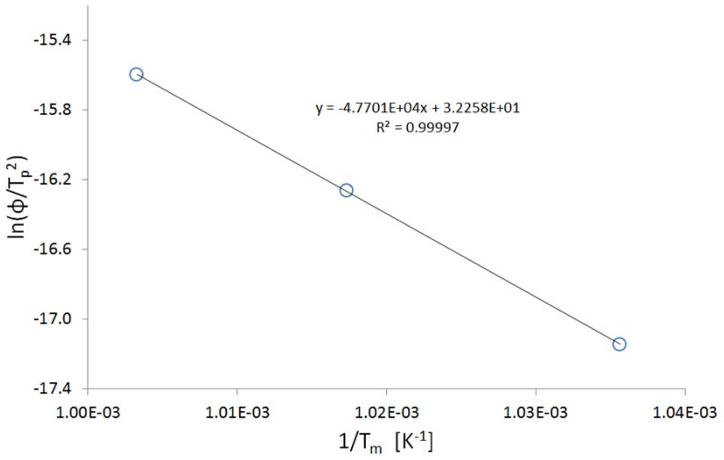

Fig. S17 Kissinger plot from DSC data. The activation energy is calculated from the slope as E_a =-47701*8.314 J·K^{-1}·mol^{-1} = 396586 J·K^{-1}·mol^{-1} = 397 kJ·K^{-1}·mol^{-1}.

The activation energy was calculated from the Kissinger plot to be E_a = 397 kJ·mol^{-1} (see Fig. S17).

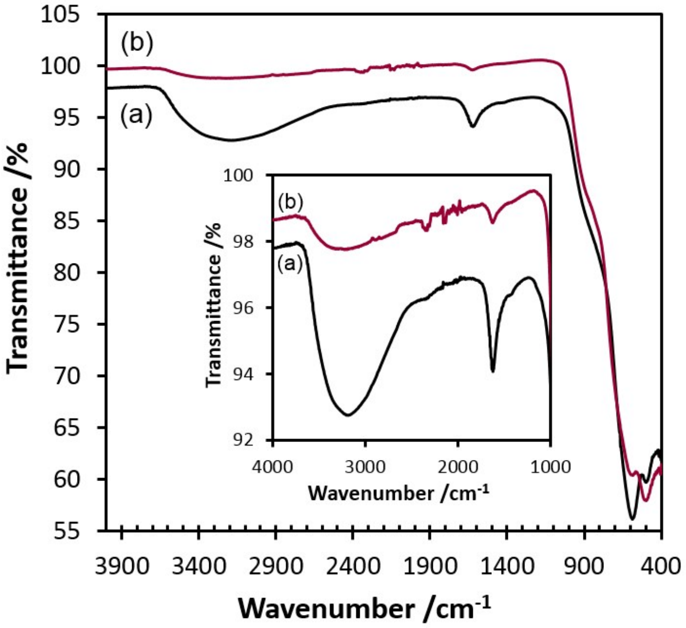

Fig. S18 FTIR spectra obtained using ATR mode from (a) d-Ta_xO_y sample and (b) L-Ta_2O_5 powder sample obtained after *in situ* heating total scattering experiments. The spectra are normalised according to the lowest transmittance point and presented with an offset.

FTIR spectra (Fig. S18) obtained before and after heating the sample to 700 °C show changes of a band around 3000-3500 cm^{-1} which is assigned to water-bridged hydroxyl groups. A second band around 1630 cm^{-1} represents H-O-H bending modes. The intensities of both water bands significantly decrease during the heating process, indicating the release of water in accord with the TG-DSC data.

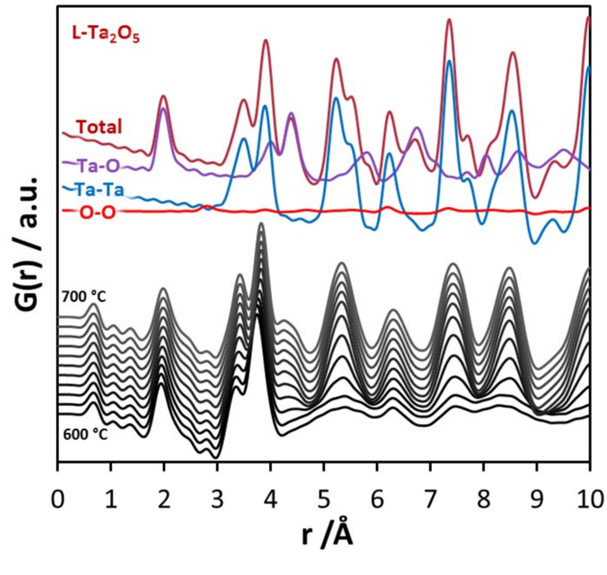

Fig. S19 Partial PDFs calculated using L-Ta_2O_5 structure described by Stephenson and Roth[S1] (Q_{max}= 22 Å^{-1}, ADPs= 0.003, delta2= 1.0, Q_{damp}= 0.0375 Å^{-1}, Q_{broad}= 4.067e-06 Å^{-1}, using PDFgui[S6]) compared to the 600-700 °C range of the PDFs obtained from *in situ* heating experiments.

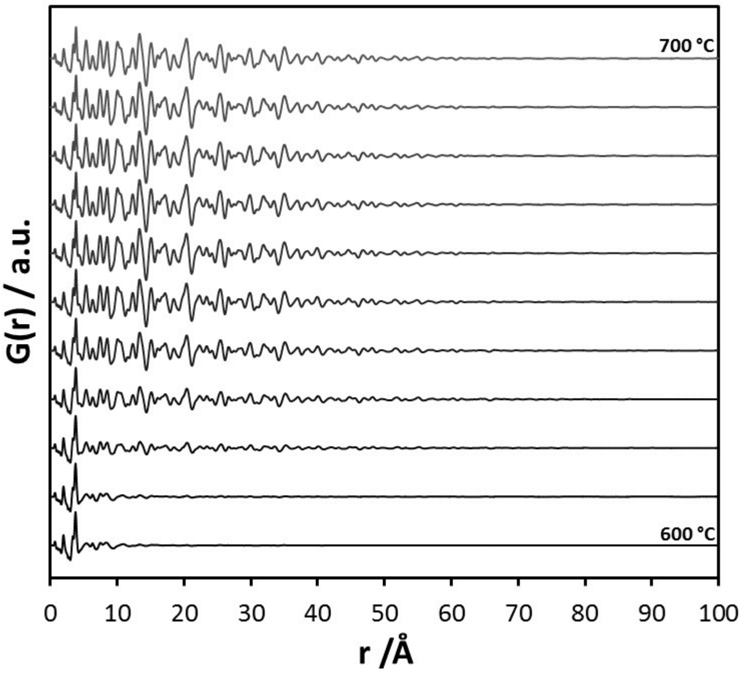

Fig. S20 Long range order in high temperature PDFs obtained from *in situ* heating experiments. PDFs were given for every 10 °C between 600 °C and 700 °C Data collected at DESY, P02.1 (Q_{max}: 22 Å^{-1}).

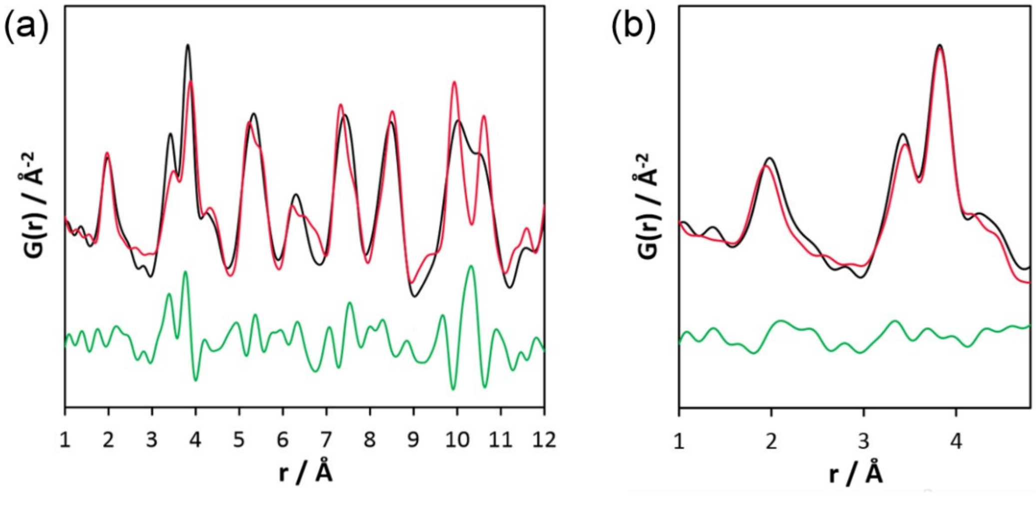

Fig. S21 Refinement of the PDF obtained at 700 °C using L-Ta_2O_5 structure[S1] carried out using PDFgui[S6] for the ranges (a) 1-12 Å and (b) 1-4.8 Å. The calculated PDF curve is plotted in red colour on top of the experimental data given in black and the difference curve is given in green colour with an offset below.

Table S1 Refined parameters for the PDF obtained at 700 °C using L-Ta_2O_5 structure (q_{max}= 22 $Å^{-1}$, q_{damp}= 0.0375 $Å^{-1}$, q_{broad}= 4.067x10^{-6} $Å^{-1}$, *fixed).

		1 - 12 Å	1 - 4.8 Å
Parameter	**Initial value**	**Refined value**	**Refined value**
Scale factor	1.000000	0.618002 (0.013)	0.701832 (0.024)
Particle diameter	70 Å	72.1653 Å	70 Å*
Quadratic corr. factor	1.0000	0.756571	0.973243
Linear corr. factor	1.0000	1.23323	1.00699
Lattice parameters /Å			
a	6.19850	6.14641	6.11537
b	40.29033	40.83900	40.0281
c	3.88850	3.86823	3.80814
ADPs			
Ta	0.0030000	0.0057508	0.0032644
O	0.0030000	0.0243903	0.0559372
Rw		0.392975	0.190979

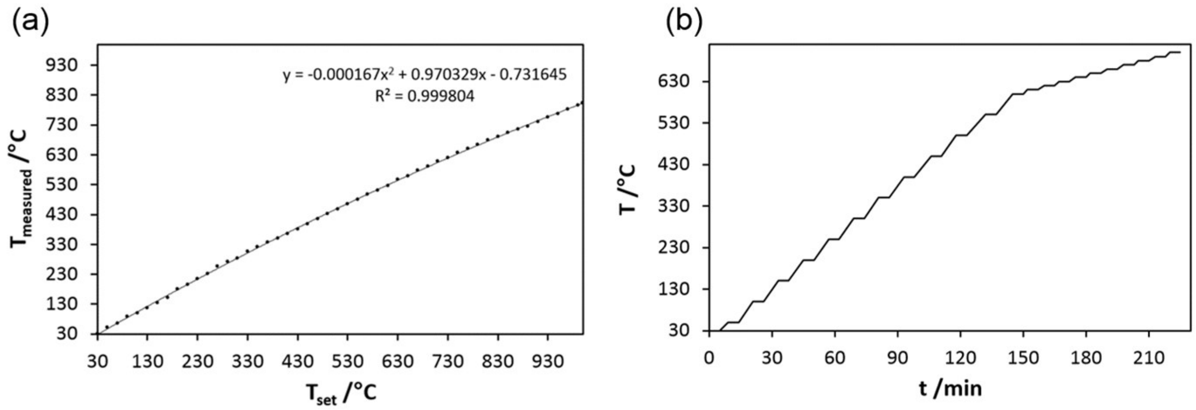

Fig. S22 (a) Temperature calibration curve used for setting the temperature for the hot air blower and (b) temperature vs. time curve for the *in situ* heating experiments. Temperature calibration was made based by inserting a thermocouple inside the empty quartz capillary heated in the same way as the samples. Data were taken for 5 min starting from 30 °C at each 50 °C in the 50-600 °C interval and at each 10 °C in the 600-700 °C interval where the heating rate was kept constant at 10 °C·min^{-1}.

Reference

S1 N.C. Stephenson and R.S. Roth, *Acta Cryst.*, 1971, **B27**, 1037.

S2 P. Juhás, C.L. Farrow, X. Yang, K.R. Knox and S.J.L. Billinge, *Acta Crystallogr.*, 2015, **A71**, 562.

S3 I. Abrahams, D.C. Bradley, H. Chudzynska, M. Motevalli and P. O´Shaughnessy, *J. Chem. Soc., Dalton Trans.*, 2000, 2685.

S4 H.E. Kissinger, *J. Res. Nat. Bur. Stand.*, 1956, **57**, 217.

S5 P. Murray and J. White, *Trans. Brit. Ceram. Soc.,* 1955, **54**, 204.

S6 C.L. Farrow, P. Juhás, J.W. Liu, D. Bryndin, E.S. Božin, J. Bloch, Th. Proffen and S.J.L. Billinge, *J. Phys.: Condens. Matter*, 2007, **19**, 335219.